

1 **Isolation and characterization of a novel *Wolbachia* bacteriophage from**
2 ***Allonemobius socius* crickets in Missouri**

3

4 Jonah Kupritz^{1#^a}, John Martin^{1,2}, Kerstin Fischer¹, Kurt C Curtis¹, Joseph R Fauver^{1#^b}, Yuefang
5 Huang¹, Young-Jun Choi¹, Wandy L Beatty³, Makedonka Mitreva^{1,2}, Peter U Fischer^{1*}

6

7 ¹ Infectious Disease Division, Washington University School of Medicine, St. Louis, Missouri,
8 United States of America

9 ² McDonnell Genome Institute, Washington University School of Medicine, St. Louis, Missouri,
10 United States of America

11 ³ Department of Molecular Microbiology, Washington University in St. Louis, St. Louis,
12 Missouri, United States of America

13 ^{#^a} Current Address: Laboratory of Parasitic Diseases, National Institute of Allergy and Infectious
14 Diseases, NIH, Bethesda, Maryland, United States of America.

15 ^{#^b} Current Address: Yale School of Public Health, New Haven, Connecticut, United States of
16 America

17

18 Corresponding author

19 E-mail: pufischer@wustl.edu

20

21

22 **Abstract**

23

24 *Wolbachia* are endosymbionts of numerous arthropod and some nematode species, are important

25 for their development and if present can cause distinct phenotypes of their hosts. Prophage DNA

26 has been frequently detected in *Wolbachia*, but particles of *Wolbachia* bacteriophages (phage

27 WO) have been only occasionally isolated. Here, we report the characterization and isolation of

28 a phage WO of the southern ground cricket, *Allonemobius socius*, and provided the first whole-

29 genome sequence of phage WO from this arthropod family outside of Asia. We screened *A.*

30 *socius* abdomen DNA extracts from a cricket population in eastern Missouri by quantitative PCR

31 for *Wolbachia* surface protein and phage WO capsid protein and found a prevalence of 55% and

32 50%, respectively, with many crickets positive for both. Immunohistochemistry using antibodies

33 against *Wolbachia* surface protein showed many *Wolbachia* clusters in the reproductive system

34 of female crickets. Whole-genome sequencing using Oxford Nanopore MinION and Illumina

35 technology allowed for the assembly of a high-quality, 55 kb phage genome containing 63 open

36 reading frames (ORF) encoding for phage WO structural proteins and host lysis and

37 transcriptional manipulation. Taxonomically important regions of the assembled phage genome

38 were validated by Sanger sequencing of PCR amplicons. Analysis of the nucleotides sequences

39 of the ORFs encoding the large terminase subunit (ORF2) and minor capsid (ORF7) frequently

40 used for phage WO phylogenetics showed highest homology to phage WOKue of the

41 Mediterranean flour moth *Ephestia kuehniella* (94.18% identity) and WOLig of the coronet

42 moth, *Craniophora ligustri* (96.86% identity), respectively. Transmission electron microscopy

43 examination of cricket ovaries showed a high density of phage particles within *Wolbachia* cells.

44 Isolation of phage WO revealed particles characterized by 40-62 nm diameter heads and up to

45 190 nm long tails. This study provides the first detailed description and genomic characterization
46 of phage WO from North America that is easily accessible in a widely distributed cricket species.

47

48 **Keywords:** *Wolbachia*, bacteriophage, arthropod, cricket, vector control

49

50

51 **Introduction**

52
53 It is estimated that 66% of all insect species and the majority of filarial parasites that infect
54 humans are infected/colonized with *Wolbachia* [1]. *Wolbachia* causes phenotypes such as
55 cytoplasmic incompatibility and feminization in arthropods, or support growth and reproduction
56 in filarial nematodes [2, 3]. *Wolbachia* is divided into several supergroups based on its *ftsZ* gene
57 sequence, with supergroups A and B found exclusively in arthropods and supergroups C and D
58 found exclusively in nematodes [4]. Active bacteriophages infecting *Wolbachia* (phage WO)
59 were first discovered in the year 2000 and remain one of few published cases of bacteriophages
60 that infect intracellular bacteria [5]. The persistence of the phage despite its documented lytic
61 activity has led to the hypothesis that phage WO provides benefit to its *Wolbachia* or arthropod
62 host [6]. Phage WO may regulate *Wolbachia* density and therefore, affect development and
63 phenotype of its eukaryotic host [7]. Further, phage WO may supply *Wolbachia* with accessory
64 genes for cytoplasmic compatibility and male killing [8].

65 In recent years, an increasing number of *Wolbachia* genomes have been sequenced and
66 phage WO is of interest for being the only known mobile genetic element in *Wolbachia*, which is
67 highly resistant to current genetic modification tools, and its hypothesized role in generating the
68 high level of diversity seen among *Wolbachia* today [6, 9]. Evidence has been provided for
69 horizontal gene transfer between *Wolbachia* strains mediated by phages WO [10]. Phages are
70 estimated to infect most of the *Wolbachia* taxa in the supergroups A and B. However, for a
71 majority of these phages, sequence data is limited to the minor capsid protein-coding gene, and
72 there remain entire families and genera of *Wolbachia*-harboring arthropods in which phage has
73 not yet been described [5]. One such example is found in crickets (*Gryllidae*) of the genus
74 *Allonemobius* (ground crickets), whose members include *A. socius* (the southern ground cricket)

75 and *A. maculatus* (the spotted ground cricket), found throughout North America. *Wolbachia*
76 belonging to supergroup B has been identified in *A. socius* (wSoc), where it is hypothesized to
77 play a role in altering the length of female crickets' spermathecal duct [11, 12]. However, phage
78 WO has neither been identified nor described in *Allonemobius*.

79 In the present study we identified, for the first time, a phage WO in *Allonemobius*
80 crickets (phage WOSoc) and estimated its prevalence. We characterized the novel phage WOSoc
81 by immunohistochemistry, transmission electron microscopy, and whole genome sequencing,
82 expanding the limited set of fully described bacteriophages of *Wolbachia* by adding this novel
83 bacteriophage for which we provide evidence of complete phage particle production, host lysis,
84 and genetic manipulation.

85
86

87 **Materials and Methods**

88

89 **Sample collection and DNA extraction**

90 Adult *A. socius* crickets (n= 40) were collected in the summer of 2019 from Forest Park, St.
91 Louis, Missouri, USA (N 38.4° 38', W 90° 17'). Crickets were sexed based on the presence
92 (female) or absence (male) of an ovipositor and ecological data including morphological features
93 and geographical distribution were used to confirm species identification. All insects were
94 euthanized by placement at -20° C for 30 minutes before dissection and homogenization of
95 abdomens in 500 µL of phosphate buffered-saline by 15-minute high-intensity beating with a 3.2
96 mm chrome Disruption Bead (BioSpec Products, Bartlesville, USA) on the Vortex-Genie 2
97 mixer (Scientific Industries, Inc., Bohemia, USA). The homogenate was spun down, and DNA
98 was prepared from the supernatant using the DNeasy Blood & Tissue Kit (Qiagen, Hilden,
99 Germany) according to manufacturer recommendations, with elution into 100 µL sterile water
100 and storage at -20°C or 4°C until use.

101 **PCR for phage and *Wolbachia* detection**

102 Conventional PCR reactions with total cricket abdomen genomic DNA template were run using
103 previously validated primers to the conserved *Wolbachia* surface protein (WSP) gene [13] and to
104 the *Wolbachia* phage capsid protein (WPCP) gene [14]. PCR was performed in 25 µL reactions
105 with 0.625 µL of 10 µM forward and reverse primers (250 nm final concentration), 2 µL DNA
106 template (2-5 ng), 12.5 µL Hot Start Taq DNA Polymerase (2X (New England Biolabs, Ipswich,
107 USA), and 9.25 µL sterile water. Following an initial 30 s denaturation at 95°C, 40 cycles were
108 run with 30 s denaturation at 95°C, 60 s annealing at 55°C, 1 min extension at 68°C, and a single
109 5 min final extension at 68°C. For each primer set and reaction, sterile water was run as a non-
110 template control. PCR products were sent to Genwiz (South Plainfield, USA) for Sanger

111 sequencing. Forward and reverse primer sequencing reactions were performed for each region of
112 interest and chromatograms were visually inspected for base call quality.

113 **Real-time PCR prevalence estimates**

114 Primer 3 software [15] was used to create qPCR-optimized WSP and WPCP primers from their
115 respective *wSoc* and *WOSoc* sequences (Table 1). For each DNA template and primer set, qPCR
116 reactions were performed in duplicate 25 µL reactions with 0.625 µL of 10 µM forward and
117 reverse primers (250 nm final concentration), 2 µL DNA template, 12.5 µL Power SYBR Green
118 Master Mix (Thermo Fisher, Waltham, USA), and 9.25 µL sterile water using the standard
119 Power SYBR Green PCR Master Mix RT-PCR Protocol (Protocol Number 436721) on a
120 QuantStudio 6 Flex Real-Time PCR System (Thermo Fisher). As positive controls for the WSP
121 and WPCP primer sets, we used 2µL Sanger-confirmed WSP- and WPCP-positive cricket
122 genomic DNA. Sterile water was run as the negative control. A conservative cycle threshold
123 (CT) cutoff value of ≤ 23 for positive determination was set for both primer sets based on
124 melting curve and relative abundance analysis corresponding to three standard deviations below
125 the negative control detection level.

126
127 **Table 1.** List of primers designed and used in the study.

Primer name	Forward primer sequence (5'→3')	Reverse primer sequence (5'– >3')	Amplicon length (bp)	Description
<i>wSoc</i>	AGATAGTGTAAACAGCGT TTTCAGGAT	CACCATAAGAACCAAAA TAACGAG	60	qPCR detection of <i>wSoc</i> in crickets
<i>WOSoc</i>	CCCTGCCTCTGTTGATCG	CCCTGCCTCTGTTGATCG	60	qPCR detection of <i>WOSoc</i> in crickets
<i>WOSoc tail</i>	CAGGTACACACCTTGTGA GTGGCG	GCCAATAATCCAGCGGCT TGTGC	6144	Region containing tail tube protein, tape measure protein, and ankyrin repeat domain
<i>WOSoc capsid</i>	TGACGTTACGGCCAATC AAGA	CTATGTGCTCGCTGTTCC TACTGGAAA	2335	<i>WOSoc</i> major and minor capsid protein genes

128
129

130 **Immunohistology for visualization of *Wolbachia***

131 For immunohistology, 10 whole *Allonemobius* crickets were fixed in 80% ethanol, embedded in
132 paraffin, and sectioned at 10 μm . Sections were stained with a monoclonal mouse antibody
133 against the *Brugia malayi* *Wolbachia* surface protein (1:100) for 1 hour at room temperature or
134 overnight at 4°C using the alkaline phosphatase-anti-alkaline-phosphatase (AAPA) technique
135 according to the manufacturer's protocol (Dako, Carpinteria, CA, USA). All antibodies were
136 diluted in TBS with 0.1% BSA. TBS with 1% albumin was used as a negative control, whereas
137 sections from *B. malayi* worms from previous studies [16] were used as positive controls,
138 respectively. After a 30 min incubation with the secondary rabbit-anti mouse IgG antibody (1:25)
139 (Dako) followed a 30 min incubation step with alkaline-phosphatase-anti-alkaline-phosphatase
140 (1:40) (Millipore Sigma, St. Louis, USA). As substrate, SIGMAFAST Fast Red TR/Naphthol
141 AS-MX (Millipore Sigma) Tablets were used, and sections were counterstained with Mayer's
142 hematoxylin (Millipore Sigma). Sections were analyzed using an Olympus-BX40 microscope
143 and photographed with an Olympus DP70 camera.

144 **DNA extraction, library preparation and whole genome sequencing.**

145 High molecular weight (HMW) DNA was purified from a homogenate of a whole single adult
146 female cricket prepared by 15 min beating with a lead bead using the MagAttract HMW DNA
147 Kit (Qiagen) according to manufacturer specifications, eluting in 100 μL sterile water. Presence
148 of HMW was confirmed by gel electrophoresis. Presence of WPCP in HMW DNA was
149 confirmed by qPCR. DNA was then purified further using AMPure XP beads (Beckman Coulter,
150 Brea, USA) at a ratio of 1.8:1 bead to DNA sample. Library was prepared according to Oxford
151 Nanopore's 1D Genomic DNA Ligation Protocol (Version GDE_9063_v109_revA) using the
152 LSK-109 Ligation Sequencing Kit (Oxford Nanopore Technologies, Cambridge, England) with
153 DNA fragments of all sizes purified using the Short Fragment Buffer. 60 μL of library

154 containing 12 μ L genomic DNA was loaded as input into the flow cell and the sequencing
155 reaction run for 20 hours using MinKNOW GUI software (Oxford Nanopore Technologies) set
156 to the High Accuracy Flip-Flop Model, generating 6.1 giga base pairs of data. Basecalling of
157 Fast5 files into Fastq format was performed using Guppy neural network basecalling software
158 [17]. Base statistics, average quality per read, sequence duplication level, and GC content were
159 assessed using FastQC software (Babraham Institute, Cambridge, UK). In parallel, genomic
160 DNA was extracted from the ovary tissue of a single cricket using Qiagen DNeasy kits as
161 described above and sequenced using a NovaSeq 6000 Sequencing System (Illumina, San Diego,
162 USA) with 2x150 bp output generating 12.2 giga base pairs of data, following qPCR
163 confirmation of phage positivity in the sample

164 **Assembly and annotation of the WOSoc genome**

165 Putative WOSoc reads were extracted by mapping MinION sequences against published phage
166 WO reference genomes using Minimap2 software [18]. Mapped reads were then mapped against
167 themselves in order to merge overlapping reads. The self-mapping output and the MinION-
168 generated Fastq sequences were input into CANU Single Molecule Sequence Assembler [19] to
169 generate a phage assembly consisting of multiple contigs. Quality trimming and adapter clipping
170 of Illumina reads was performed using Trimmomatic [20]. The PRICE assembly tool [21] was
171 used to extend existing contigs using the Illumina data. Redundans was used collapse redundant
172 contigs, scaffold contigs, and close gaps using both the Oxford Nanopore Technologies (ONT)
173 reads and Illumina reads. ONT reads were error-corrected using FMLRC [22] before feeding
174 them into the Redundans pipeline [23]. We then manually curated the assembly and corrected
175 assembly errors. Finally, Pilon automated genome assembly improvement pipeline [24] was used
176 to polish the assembly and reduce base-call errors. Annotation of the assembled phage genome
177 was performed using the Rapid Annotation Using Subsystem Technology Toolkit (RASTtk)

178 SEED-based prokaryotic genome annotation engine with default presets, which has established
179 validity for annotating phage genomes [25, 26], identifying genomic “features” (protein-coding
180 genes and RNA). Genomic features were visualized in scaffolds independently and manually
181 color-coded by function using Gene Graphics visualization application [27].

182 **PCR and Sanger sequencing for genome verification**

183 Primers were manually designed to amplify phage tail and capsid regions based on the MinION
184 reads (Table 1). Conventional PCR reactions were run with these primers and cricket abdomen
185 DNA as described previously with a 60°C annealing temperature for both primer sets. Amplicons
186 were gel-excised, purified, and 3730 Sanger sequenced.

187 **Phylogenetic analyses**

188 DNA sequences of phage WO open reading frames 2 (ORF2) and 7 (ORF7), respectively coding
189 for the large terminase subunit and minor capsid, are biomarkers known to produce highly
190 congruent phage WO phylogenies [5]. Nucleotide sequences of ORF2 and ORF7 of WOSoc
191 were compared to published gene sequences in NCBI Genbank. Phylogenetic trees were
192 generated based on WOSoc ORF2 and ORF7 identity to the top 4 BLAST hits based on pairwise
193 alignments using the NCBI BLAST Tree View Neighbor-Joining tree method with distances
194 from the node computed by NCBI presets. ORF2 sequence was extracted from Scaffold 1 of the
195 phage assembly, while the entire ORF7 gene was provided by Sanger sequencing of the capsid
196 region as described above.

197 **Phage particle purification**

198 Phage was purified according to the protocol described in [28] with slight modification. Unless
199 otherwise noted, all reagents were purchased from Sigma-Aldrich, St. Louis, USA. Complete
200 mature *A. socius* males and females (N = 70) were euthanized and thoroughly homogenized in 40
201 mL of SM buffer (50 mM Tris-HCL, pH 7.5, 0.1 M NaCl, 10 mM MgSO₄ • 7 H₂O and 0.1% w/v

202 gelatin containing 1 µg/mL RNase A). Homogenate was incubated on ice for 1 hour followed by
203 11,000xg centrifugation for 10 minutes at 4°C to remove debris. Solid polyethylene glycol (PEG)
204 was added to homogenate to a final concentration of 10% and mixed by manual shaking for 1
205 minute, followed by an additional 1-hour incubation on ice and 11,000xg centrifugation for 10
206 minutes at 4°C. Supernatant was discarded and the remaining pellet was resuspended in 10 mL of
207 SM buffer. To the suspension, an equal volume of chloroform was added followed by
208 centrifugation at 3,000xg for 15 minutes at 4°C to remove the PEG. The aqueous layer
209 containing phage was filtered through a 0.22 µM vacuum filter to remove *Wolbachia* and other
210 bacteria. Phage lysate was concentrated using Amicon Ultra-15 100 kDA Centrifugal Units
211 (Millipore, Burlington, USA) according to [29] and reconstituted in a final volume of 1 mL of
212 SM buffer.

213 **Transmission electron microscopy (TEM) for visualization of WOSoc particles**

214 From freshly caught adult female *A. socius*, ovaries were dissected and adsorbed to an electron
215 transparent sample support (EM) grid. Tissue was washed in PBS and fixed in 1%
216 glutaraldehyde for 5 minutes at room temperature, followed by two 30-second washes with
217 deionized water. Phage particles were negatively stained in 1% uric acid for 1 minute and wicked
218 gently and placed in a grid box to dry. Phage suspension was processed identically, with 50 µL
219 of the concentrated suspension adsorbed to an EM grid. Samples were observed on a JEOL 1200
220 EX transmission electron microscope (JEOL USA Inc., Peabody, USA) equipped with an AMT
221 8-megapixel digital camera (Advanced Microscopy Techniques, Woburn, USA)
222 To confirm the presence of phage in *Wolbachia* by TEM, one half of the ovaries of each of 6
223 crickets was fixed in 2% paraformaldehyde/2.5% glutaraldehyde (Polysciences Inc., Warrington,
224 USA) in 100 mM phosphate buffer, pH 7.2, for 1 hour at room temperature. The other half of the
225 ovary sample was added to 1X PBS for DNA extraction and confirmation of *Wolbachia* presence

226 by PCR. Only samples that were positive by PCR for Wolbachia were further processed for
227 TEM. These samples were washed in phosphate buffer and post-fixed in 1% osmium tetroxide
228 (Polysciences Inc.) for 1 hour. Samples were then rinsed extensively in distilled water prior to
229 staining with 1% aqueous uranyl acetate (Ted Pella Inc., Redding, USA) for 1 hour. Following
230 several rinses in distilled water, samples were dehydrated in a graded series of ethanol and
231 embedded in Eponate 12 resin (Ted Pella Inc.). Sections of 95 nm were cut with a Leica Ultracut
232 UCT ultramicrotome (Leica Microsystems Inc., Bannockburn, USA), stained with uranyl acetate
233 and lead citrate, and viewed on a JEOL 1200 EX transmission electron microscope (JEOL USA
234 Inc.) equipped with an AMT 8-megapixel digital camera (Advanced Microscopy Techniques)
235 [30].

236
237

238 **Results**

239

240 **Prevalence of Phage WO and *Wolbachia* in *A. socius***

241 DNA encoding WSP was used as a marker for assessing the prevalence of *Wolbachia* in crickets.

242 In order to confirm the DNA sequence of WSP of Missouri crickets, DNA was amplified by

243 conventional PCR using the pre-validated WSP primers. WSP sequence showed 100% identity

244 to WSP of *A. socius* from Virginia (Accession: AY705236.1, data not shown). A 400 bp

245 amplicon of phage DNA was amplified by conventional PCR using pre-validated primers

246 corresponding to nucleotide positions 7353-7761 of phage WO of cricket *Teleogryllus*

247 *taiwanemma* cricket and showed close homology to the capsid protein genes from phage WO of

248 *Supella longipalpa* (95.50% identity, 100% query coverage, Accession: KR911861.1) and *Cadra*

249 *cautella* (94.50% identity, 100% query coverage, Accession: AB478515.1). The *A. socius* WSP

250 and phage WOSoc WPCP gene sequences were used to design SYBR-based real-time PCR

251 assays for WSP and WPCP, respectively. Using the strict CT cutoff of 23 cycles, we determined

252 that from 40 insects sampled 19 (47.5%) were positive for both WPCP and WSP DNA via qPCR

253 with our optimized primers; three samples (7.5%) were WSP-positive but WPCP-negative.

254 Confirmation of the *Wolbachia* prevalence results was done using an orthogonal
255 approach, i.e. visualization by immunohistology. Endobacteria were found in about 50% of the
256 female crickets. They were detected throughout the abdomen, however density was highest in the
257 reproductive tract (Fig. 1). *Wolbachia* were detected in distinct, but varying parts of the panoistic
258 ovarioles. In the apical part of the ovariole, *Wolbachia* were seen in the inner section of the
259 follicle epithelium (Fig. 1C), but in more mature eggs, these cells are devoid of *Wolbachia* and
260 endobacteria were concentrated in large numbers in one pole of the egg cell (Fig. 1F). The high
261 density of *Wolbachia* in developing eggs ensures transovarial transmission of *Wolbachia* and

262 phage WO [31]. It is expected that in this context, where *Wolbachia* negatively impacts its host's
263 fitness, host selection will act to limit or eliminate the endosymbiont, which may explain the less
264 than ubiquitous *wSoc* prevalence. At the same time, high phage density favors the insect host in a
265 parasitic *Wolbachia* context, which benefits from the reduction in *Wolbachia* density resulting
266 from phage-mediated lysis or transcriptional regulation, which could promote phage abundance
267 to the high levels seen in *wSoc*-infected insects [6].

268
269 **Table 2.** Prevalence estimates of *Wolbachia* surface protein (WSP) and phage capsid protein
270 (WPCP) DNA in *Allonemobius socius* crickets from Missouri.

		WSP		Total N (%)
		Positive N (%)	Negative N (%)	
WPCP	Positive N (%)	19 (47.5%)	1 (2.5%)	20 (50%)
	Negative N (%)	3 (7.5%)	17 (42.5%)	20 (50%)
	Total N (%)	22 (55%)	18 (45%)	40 (100%)

271 Estimates are based on a SYBR qPCR assay with a strict cutoff of $CT \leq 23$ in 40 adult *A. socius*
272 abdomen genomic DNA extracts.

273
274
275 **Figure 1. Immunohistological localization of *wSoc*.** Black arrows indicate *Wolbachia* (red). **A.**
276 Posterior abdomen containing intestinal tissue and oviduct containing *Wolbachia* (200 μ m). **B.**
277 Ovary tissue showing dense clusters of *Wolbachia* at the site of maturing oocytes (200 μ m). **C.**
278 *Wolbachia* localized to the follicle epithelium. **D** (50 μ m), **E**, and **F**. Close-up of oocytes in the
279 female cricket oviduct showing *Wolbachia* cells in studding follicles. The nucleus (GV) is visible
280 in the upper oocyte in **F**. (20 μ m) Abbreviations: FE = follicle epithelium; od = oviduct; ov =
281 ovaries; GV = germinal vesicle. Scale bar: 10 μ m.
282

283 **Isolation and visualization of Phage WO of *A. socius***

284 Although we detected capsid DNA of phage WO in most *Wolbachia*-positive *A. socius* samples,
285 it was theoretically possible that this was exclusively prophage DNA incorporated into the

286 genome of *Wolbachia* and that no phage particles were formed. Therefore, we used TEM to
287 visualize particles of phage WO of *A. socius*. Several intracellular *Wolbachia*-containing
288 stereotypical hexagonal phage particles were detected in ovarian tissue (Fig. 2). Small clusters of
289 *Wolbachia* cells that contained up to 30 complete phage particles per cells were observed to
290 mature egg cells (Fig 2. A, B, D). TEM examination of the filtrate from phage precipitation
291 revealed numerous phage WO particles. Measurement of 10 particles showed an average
292 diameter of the icosahedral head structure of 47 and 62 nm (\pm x nm SD) and 175 and 135nm
293 long, striated tails (Fig 2. E, F).

294

295 **Figure 2. Transmission electron microscopy (TEM) of WOSoc particles.** **A.** Clusters of
296 intracellular *Wolbachia* wSoc (arrows) in the ovary of *A. socius* (scale bar 2 μ m). **B.** Densely
297 packed phages WOSoc (arrows) inside a *Wolbachia* endobacterium (scale bar 500 nm). **C.** and
298 **D.** Compact, electron dense hexagonal arrays of phages WOSoc (arrows) in *Wolbachia* (scale
299 bar 500 nm). **E.** and **F.** Complete, purified phage particles with 47 to 62 nm capsids (arrow) and
300 175 to 130 nm tails (arrow head, scale bar 100 nm). Abbreviations: ov, ovaries; W, *Wolbachia*,
301 rER, rough endoplasmic reticulum; m, mitochondrion.

302

303

304 **The WOSoc genome indicates potential for lysis and transcriptional manipulation of the
305 host**

306 Following the detection of phage DNA in WSP-positive crickets and the demonstration of
307 distinct phage particles, we set out to genomically characterize the novel phage WO to gain
308 insight into its lytic potential and its similarity to known phages WO. Using the well-
309 characterized genome of WOVitA1 (a *Wolbachia* bacteriophage found in the parasitic wasp,
310 *Nasonia vitripennis*) as a reference genome, we identified 511 homologous WOSoc reads from
311 the MinION run of whole-cricket homogenate HMW DNA with an average quality per read
312 (Phred Score) of 23, corresponding to an overall base call accuracy exceeding 99%. From these
313 reads, we assembled 12 contigs totaling 53,916 bp at an average depth of 14.6X and a GC

314 content of 35%. After confirming and extending these contigs with Illumina reads and removing
315 low quality reads and reads derived from the *Wolbachia* genome, the WOSoc genome was
316 captured in 4 high-quality scaffolds totaling 55,288 bp. To further validate our assembly, we
317 Sanger sequenced PCR-amplified phage sequence from taxonomically important phage regions
318 using primers generated from the scaffolds, collectively representing nearly one-eighth of the
319 assembly including a continuous, 6,144 bp contig containing complete open reading frames for
320 tail morphogenesis proteins and a 2,289 bp region encoding the major and minor capsid proteins
321 and head decoration protein (all sequence data are available in Supplementary File S1 and the
322 assembly is available in GenBank under the accession IDs MD788653-MW788656). RASTtk
323 annotation identified 63 features which included 33 described and 30 hypothetical or unidentified
324 ORFs based on similarity and bidirectional best hit computation (see Supplementary File S2 for a
325 complete list of these features including full-length protein and gene sequences). Of the 33
326 described ORFs, over half (N = 17) encoded structural features including tail (N = 9), head (N =
327 5), and baseplate (N = 3) assembly. We also identified genes necessary for phage replication (N
328 = 2), *Wolbachia* cell wall lysis (N = 3), and a resolvase protein which may catalyze site-specific
329 bacteriophage DNA integration [32] (Fig. 3). Strikingly, we found five features which may
330 regulate *Wolbachia* host transcriptional processes including N-acetylglucosamine-1-phosphate
331 uridyltransferase, which may regulate *Wolbachia* transcription by altering glutamine synthetase
332 activity [33] and glycosyl transferase, which is known to protect phages from bacterial
333 endonucleases [34]. Collectively, these features suggest that WOSoc is an active particle-
334 forming phage with potential for lytic and lysogenic behavior, reflecting an intimate interaction
335 with its bacterial host.

336

337 **Figure 3. Annotation of the WOSoc genome.** 63 features from the RASTk annotation of the 4-
338 scaffold WOSoc assembly are displayed: ankyrin repeats (N = 2), baseplate assembly (N = 3),
339 phage head (N = 5), integration into *Wolbachia*'s genome (N = 2), lysis of *Wolbachia* cells (N =
340 3), protection from *Wolbachia* endonucleases (N = 1), DNA replication and mismatch repair (N
341 = 2), tail formation (N = 9), transcriptional regulation (N = 5), virulence (N = 1), undescribed
342 hypothetical proteins (N = 30). Abbreviations: NAMLA = N-acetylmuramoyl-L-alanine
343 amidase; ANK = ankyrin. Scale bars: 1 kb within their respective scaffolds.
344
345

346 **Phylogenetic analysis of WOSoc suggests a close relationship with phages WO of moths**

347 In order to compare phage WOSoc to a larger number of phage WO for which the complete
348 genome sequence is not available, we performed pairwise comparison with published ORF2 and
349 ORF7 phage WO sequences. Phage WOSoc ORF2 showed the highest homology to phage
350 WOKue of the Mediterranean flour moth *Ephestia kuehniella* (94.18% nucleotide identity, 100%
351 query coverage, Accession: AB036666.1), while phage WOSoc ORF7 was most similar to
352 WOLig of the coronet moth, *Craniophora ligustri* (96.86% nucleotide identity, 100% query
353 cover, Accession: LR990976.1), both insects of the order Lepidoptera. (Fig. 4). High homology
354 (> 99% identity), which is not uncommon for known conserved phage element sequences, such
355 as the large terminase subunit or the minor capsid protein region, was not observed.
356

357 **Figure 4. Phylogenetic comparison of WOSoc with published phage sequences**

358 Neighbor-joining trees generated from published phage WO nucleotide sequences aligned to
359 WOSoc **A.** Large terminase subunit (ORF2), showing homology to WOKue of the moth
360 *Ephestia kueniella* and **B.** minor capsid protein (ORF7), showing high homology to WOLig of
361 the moth *Craniophora ligustri*. Scale bars denote distance from the node as calculated by the
362 NCBI Tree View software.
363
364

365 **Discussion**

366
367 The present study identified for the first time a particle-forming phage WO in North American
368 crickets and provided the whole genome sequence of phage WOSoc. About half of female *A.*
369 *socius* crickets screened by PCR contained *Wolbachia*. Within arthropod populations, *Wolbachia*
370 infection prevalence closely resembled that seen in other supergroup B infected species [35-38].
371 More than 85% of *Wolbachia*-positive crickets were also positive for phage WO DNA,
372 indicating co-transmission of *Wolbachia* and phage WO. In a DNA extract of one cricket, we
373 detected phage WO DNA, but not *Wolbachia* DNA. This may be due to contamination with
374 DNA from a phage-positive sample or more likely due to failure of the assay to pick up very low
375 amounts of *Wolbachia* DNA, since a single *Wolbachia* cell may contain many genomes of phage
376 WO. Our TEM examination of *Wolbachia* illustrated this very nicely.

377 Immunohistological detection of *Wolbachia* in *A. socius* showed high densities of
378 endobacteria in maturing egg cells. TEM examination of ovaries of *A. socius* revealed numerous
379 phage WO particles arranging in varying structures within the *Wolbachia* cells. Occasionally,
380 intracellular, electron-dense, hexagonal arrays where detected that could be the product of phage
381 WOSoc self-assembly into ordered nanoarrays as seen in other bacteriophages [39]. Little
382 information is available that describes the ultrastructure of assembled phage WO particles within
383 *Wolbachia*, however the observed morphology of isolated phage WOSoc particles is similar to
384 other isolated phage WO particles [40-42].

385 Genomic evidence showed the potential of complete phage WOSoc particle formation
386 and validated the morphology results. Previous reports link the presence of prophage WO DNA
387 with host phenotypes [43, 44]. However, our study showed not only the presence of prophage
388 WO DNA, but also demonstrates particle formation and active propagation of phage WOSoc.

389 Phage particles are the driver of genetic elements into new *Wolbachia* strains. Bacteriophages are
390 considered to be relatively host-specific, but potential host species can be predicted based on
391 sequences of annotated receptor-binding proteins [45]. Unfortunately, these sequences are not
392 always available and further experimental studies have to elucidate the host range of phage
393 WOSoc and its potential to genetically manipulate *Wolbachia*. The isolation of phage WOSoc
394 offers exciting possibilities for understanding the evolutionary and current role of *Wolbachia*'s
395 only known mobile genetic element and an active regulator of *Wolbachia* density on the
396 endosymbiont-induced characteristics such as cytoplasmic incompatibility and reproductive
397 support. Future studies may show whether phage WOSoc plays a role in the spermathecal duct
398 shortening which is a well-documented effect of *Wolbachia* in *Allonemobius* genus crickets [11].

399 So far, there are only a handful of complete phage WO genome sequences available in
400 the public databases, and this study has expanded the list by adding a validated 55 kilobase
401 genome of phage WOSoc. Like closely related active phage WO of *Cadra cautella*, WOSoc
402 contains intact open reading frames encoding proteins essential to phage particle formation,
403 including tail morphogenesis and DNA packaging, which are absent in inactive, prophages of
404 *Wolbachia* [46].

405 *Wolbachia* are considered as targets for alternative chemotherapy of human filariasis,
406 caused by parasitic nematodes [47] and as alternative tools for vector control [48]. Therefore, a
407 better understanding of the role of phage WO in regulating *Wolbachia* populations is important
408 to optimize these intervention strategies. In addition, our discovery of a novel phage WO in a
409 common and easily accessible insect species, may help to add *Wolbachia* to the list of bacteria
410 that can be targeted by phage therapy. The concept of phage therapy is old, but has gained new
411 interest in recent years by the rapid increase of antimicrobial resistance [49]. Future studies are

412 needed to show whether phage WOSoc can be utilized to manipulate *Wolbachia* in *A. socius* or
413 other host species infected by *Wolbachia*.

414

415 **Supporting Information**

416 S1 Assembly of the genome of phage wAsoc and selected confirmed DNA sequences used for
417 phylogenetic analysis.

418 S2 Annotation of the genome of phage wAsoc.

419

420 **Acknowledgements**

421 The authors would like to thank Dr. Gary Weil for his support. The study was funded in part by
422 The Foundation for Barnes Jewish Hospital. JK was supported by the Washington University
423 Biology Summer Undergraduate Research Fellowship Program (BIOSURF).

424

425 **References**

426

- 427 1. Hilgenboecker K, Hammerstein P, Schlattmann P, Telschow A, Werren JH. How many
428 species are infected with Wolbachia?--A statistical analysis of current data. FEMS Microbiol
429 Lett. 2008;281(2):215-20. Epub 2008/03/04. doi: 10.1111/j.1574-6968.2008.01110.x. PubMed
430 PMID: 18312577; PubMed Central PMCID: PMCPMC2327208.
- 431 2. Taylor MJ, Bandi C, Hoerauf A. Wolbachia bacterial endosymbionts of filarial
432 nematodes. Adv Parasitol. 2005;60:245-84. Epub 2005/10/19. doi: 10.1016/S0065-
433 308X(05)60004-8. PubMed PMID: 16230105.
- 434 3. Duplouy A, Couchoux C, Hanski I, van Nouhuys S. Wolbachia Infection in a Natural
435 Parasitoid Wasp Population. PLoS One. 2015;10(8):e0134843. Epub 2015/08/06. doi:
436 10.1371/journal.pone.0134843. PubMed PMID: 26244782; PubMed Central PMCID:
437 PMCPMC4526672.
- 438 4. Lo N, Casiraghi M, Salati E, Bazzocchi C, Bandi C. How many wolbachia supergroups
439 exist? Mol Biol Evol. 2002;19(3):341-6. Epub 2002/02/28. doi:
440 10.1093/oxfordjournals.molbev.a004087. PubMed PMID: 11861893.
- 441 5. Gavotte L, Henri H, Stouthamer R, Charif D, Charlat S, Bouletreau M, et al. A Survey of
442 the bacteriophage WO in the endosymbiotic bacteria Wolbachia. Mol Biol Evol. 2007;24(2):427-
443 35. Epub 2006/11/11. doi: 10.1093/molbev/msl171. PubMed PMID: 17095536.

444 6. Kent BN, Bordenstein SR. Phage WO of Wolbachia: lambda of the endosymbiont world.
445 Trends Microbiol. 2010;18(4):173-81. Epub 2010/01/20. doi: 10.1016/j.tim.2009.12.011.
446 PubMed PMID: 20083406; PubMed Central PMCID: PMCPMC2862486.

447 7. Tanaka K, Furukawa S, Nikoh N, Sasaki T, Fukatsu T. Complete WO phage sequences
448 reveal their dynamic evolutionary trajectories and putative functional elements required for
449 integration into the Wolbachia genome. Appl Environ Microbiol. 2009;75(17):5676-86. Epub
450 2009/07/14. doi: 10.1128/AEM.01172-09. PubMed PMID: 19592535; PubMed Central PMCID:
451 PMCPMC2737910.

452 8. Kaur RS, J.D.; L. Cross, K.; Leigh, B.; J. Mansueto, A.; Stewart, V.; R. Bordenstein, S.;
453 R. Bordenstein, S. . Living in the Endosymbiotic World of Wolbachia: A Centennial Review.
454 Preprints. 2021.

455 9. Wang N, Jia S, Xu H, Liu Y, Huang D. Multiple Horizontal Transfers of Bacteriophage
456 WO and Host Wolbachia in Fig Wasps in a Closed Community. Front Microbiol. 2016;7:136.
457 Epub 2016/02/26. doi: 10.3389/fmicb.2016.00136. PubMed PMID: 26913026; PubMed Central
458 PMCID: PMCPMC4753557.

459 10. Wang GH, Sun BF, Xiong TL, Wang YK, Murfin KE, Xiao JH, et al. Bacteriophage WO
460 Can Mediate Horizontal Gene Transfer in Endosymbiotic Wolbachia Genomes. Front Microbiol.
461 2016;7:1867. Epub 2016/12/15. doi: 10.3389/fmicb.2016.01867. PubMed PMID: 27965627;
462 PubMed Central PMCID: PMCPMC5126046.

463 11. Marshall JL. Rapid evolution of spermathecal duct length in the Allonemobius socius
464 complex of crickets: species, population and Wolbachia effects. PLoS One. 2007;2(8):e720.
465 Epub 2007/08/09. doi: 10.1371/journal.pone.0000720. PubMed PMID: 17684565; PubMed
466 Central PMCID: PMCPMC1934930.

467 12. Marshall JL. The Allonemobius-Wolbachia host-endosymbiont system: evidence for
468 rapid speciation and against reproductive isolation driven by cytoplasmic incompatibility.
469 Evolution. 2004;58(11):2409-25. Epub 2004/12/23. doi: 10.1111/j.0014-3820.2004.tb00871.x.
470 PubMed PMID: 15612285.

471 13. Fischer P, Schmetz C, Bandi C, Bonow I, Mand S, Fischer K, et al. Tunga penetrans:
472 molecular identification of Wolbachia endobacteria and their recognition by antibodies against
473 proteins of endobacteria from filarial parasites. Exp Parasitol. 2002;102(3-4):201-11. Epub
474 2003/07/15. doi: 10.1016/s0014-4894(03)00058-4. PubMed PMID: 12856318.

475 14. Masui S, Kamoda S, Sasaki T, Ishikawa H. Distribution and evolution of bacteriophage
476 WO in Wolbachia, the endosymbiont causing sexual alterations in arthropods. J Mol Evol.
477 2000;51(5):491-7. Epub 2000/11/18. doi: 10.1007/s002390010112. PubMed PMID: 11080372.

478 15. Untergasser A, Cutcutache I, Koressaar T, Ye J, Faircloth BC, Remm M, et al. Primer3--
479 new capabilities and interfaces. Nucleic Acids Res. 2012;40(15):e115. Epub 2012/06/26. doi:
480 10.1093/nar/gks596. PubMed PMID: 22730293; PubMed Central PMCID: PMCPMC3424584.

481 16. Fischer K, Beatty WL, Jiang D, Weil GJ, Fischer PU. Tissue and stage-specific
482 distribution of Wolbachia in *Brugia malayi*. PLoS Negl Trop Dis. 2011;5(5):e1174. Epub
483 2011/06/02. doi: 10.1371/journal.pntd.0001174. PubMed PMID: 21629728; PubMed Central
484 PMCID: PMCPMC3101188.

485 17. Wick RR, Judd LM, Holt KE. Performance of neural network basecalling tools for
486 Oxford Nanopore sequencing. Genome Biol. 2019;20(1):129. Epub 2019/06/27. doi:
487 10.1186/s13059-019-1727-y. PubMed PMID: 31234903; PubMed Central PMCID:
488 PMCPMC6591954.

489 18. Li H. Minimap and miniasm: fast mapping and de novo assembly for noisy long
490 sequences. *Bioinformatics*. 2016;32(14):2103-10. Epub 2016/05/07. doi:
491 10.1093/bioinformatics/btw152. PubMed PMID: 27153593; PubMed Central PMCID:
492 PMCPMC4937194.

493 19. Koren S, Walenz BP, Berlin K, Miller JR, Bergman NH, Phillippy AM. Canu: scalable
494 and accurate long-read assembly via adaptive k-mer weighting and repeat separation. *Genome*
495 *Res*. 2017;27(5):722-36. Epub 2017/03/17. doi: 10.1101/gr.215087.116. PubMed PMID:
496 28298431; PubMed Central PMCID: PMCPMC5411767.

497 20. Bolger AM, Lohse M, Usadel B. Trimmomatic: a flexible trimmer for Illumina sequence
498 data. *Bioinformatics*. 2014;30(15):2114-20. Epub 2014/04/04. doi:
499 10.1093/bioinformatics/btu170. PubMed PMID: 24695404; PubMed Central PMCID:
500 PMCPMC4103590.

501 21. Ruby JG, Bellare P, Derisi JL. PRICE: software for the targeted assembly of components
502 of (Meta) genomic sequence data. *G3 (Bethesda)*. 2013;3(5):865-80. Epub 2013/04/04. doi:
503 10.1534/g3.113.005967. PubMed PMID: 23550143; PubMed Central PMCID:
504 PMCPMC3656733.

505 22. Wang JR, Holt J, McMillan L, Jones CD. FMLRC: Hybrid long read error correction
506 using an FM-index. *BMC Bioinformatics*. 2018;19(1):50. Epub 2018/02/11. doi:
507 10.1186/s12859-018-2051-3. PubMed PMID: 29426289; PubMed Central PMCID:
508 PMCPMC5807796.

509 23. Prysucz LP, Gabaldon T. Redundans: an assembly pipeline for highly heterozygous
510 genomes. *Nucleic Acids Res*. 2016;44(12):e113. Epub 2016/05/01. doi: 10.1093/nar/gkw294.
511 PubMed PMID: 27131372; PubMed Central PMCID: PMCPMC4937319.

512 24. Walker BJ, Abeel T, Shea T, Priest M, Abouelliel A, Sakthikumar S, et al. Pilon: an
513 integrated tool for comprehensive microbial variant detection and genome assembly
514 improvement. *PLoS One*. 2014;9(11):e112963. Epub 2014/11/20. doi:
515 10.1371/journal.pone.0112963. PubMed PMID: 25409509; PubMed Central PMCID:
516 PMCPMC4237348.

517 25. Brettin T, Davis JJ, Disz T, Edwards RA, Gerdes S, Olsen GJ, et al. RASTtk: a modular
518 and extensible implementation of the RAST algorithm for building custom annotation pipelines
519 and annotating batches of genomes. *Sci Rep*. 2015;5:8365. Epub 2015/02/11. doi:
520 10.1038/srep08365. PubMed PMID: 25666585; PubMed Central PMCID: PMCPMC4322359.

521 26. McNair K, Aziz RK, Pusch GD, Overbeek R, Dutilh BE, Edwards R. Phage Genome
522 Annotation Using the RAST Pipeline. *Methods Mol Biol*. 2018;1681:231-8. Epub 2017/11/15.
523 doi: 10.1007/978-1-4939-7343-9_17. PubMed PMID: 29134599.

524 27. Harrison KJ, Crecy-Lagard V, Zallot R. Gene Graphics: a genomic neighborhood data
525 visualization web application. *Bioinformatics*. 2018;34(8):1406-8. Epub 2017/12/12. doi:
526 10.1093/bioinformatics/btx793. PubMed PMID: 29228171; PubMed Central PMCID:
527 PMCPMC5905594.

528 28. Fujii Y, Kubo T, Ishikawa H, Sasaki T. Isolation and characterization of the
529 bacteriophage WO from Wolbachia, an arthropod endosymbiont. *Biochem Biophys Res*
530 *Commun*. 2004;317(4):1183-8. Epub 2004/04/20. doi: 10.1016/j.bbrc.2004.03.164. PubMed
531 PMID: 15094394.

532 29. Bonilla N, Rojas MI, Netto Flores Cruz G, Hung SH, Rohwer F, Barr JJ. Phage on tap-a
533 quick and efficient protocol for the preparation of bacteriophage laboratory stocks. *PeerJ*.

534 2016;4:e2261. Epub 2016/08/23. doi: 10.7717/peerj.2261. PubMed PMID: 27547567; PubMed
535 Central PMCID: PMCPMC4975003.

536 30. Fischer K, Beatty WL, Weil GJ, Fischer PU. High pressure freezing/freeze substitution
537 fixation improves the ultrastructural assessment of Wolbachia endosymbiont-filarial nematode
538 host interaction. *PLoS One*. 2014;9(1):e86383. Epub 2014/01/28. doi:
539 10.1371/journal.pone.0086383. PubMed PMID: 24466066; PubMed Central PMCID:
540 PMCPMC3895037.

541 31. Genty LM, Bouchon D, Raimond M, Bertaux J. Wolbachia infect ovaries in the course of
542 their maturation: last minute passengers and priority travellers? *PLoS One*. 2014;9(4):e94577.
543 Epub 2014/04/12. doi: 10.1371/journal.pone.0094577. PubMed PMID: 24722673; PubMed
544 Central PMCID: PMCPMC3983217.

545 32. Thorpe HM, Smith MC. In vitro site-specific integration of bacteriophage DNA catalyzed
546 by a recombinase of the resolvase/invertase family. *Proc Natl Acad Sci U S A*.
547 1998;95(10):5505-10. Epub 1998/05/20. doi: 10.1073/pnas.95.10.5505. PubMed PMID:
548 9576912; PubMed Central PMCID: PMCPMC20407.

549 33. Rhee SG, Park SC, Koo JH. The role of adenylyltransferase and uridylyltransferase in the
550 regulation of glutamine synthetase in *Escherichia coli*. *Curr Top Cell Regul*. 1985;27:221-32.
551 Epub 1985/01/01. doi: 10.1016/b978-0-12-152827-0.50026-8. PubMed PMID: 2868842.

552 34. Markine-Goriaynoff N, Gillet L, Van Etten JL, Korres H, Verma N, Vanderplasschen A.
553 Glycosyltransferases encoded by viruses. *J Gen Virol*. 2004;85(Pt 10):2741-54. Epub
554 2004/09/28. doi: 10.1099/vir.0.80320-0. PubMed PMID: 15448335.

555 35. Lis A, Maryanska-Nadachowska A, Kajtoch L. Relations of Wolbachia Infection with
556 Phylogeography of *Philaenus spumarius* (Hemiptera: Aphrophoridae) Populations Within and
557 Beyond the Carpathian Contact Zone. *Microb Ecol*. 2015;70(2):509-21. Epub 2015/02/15. doi:
558 10.1007/s00248-015-0570-2. PubMed PMID: 25681033; PubMed Central PMCID:
559 PMCPMC4494152.

560 36. Zhang D, Zhan X, Wu X, Yang X, Liang G, Zheng Z, et al. A field survey for Wolbachia
561 and phage WO infections of *Aedes albopictus* in Guangzhou City, China. *Parasitol Res*.
562 2014;113(1):399-404. Epub 2013/11/14. doi: 10.1007/s00436-013-3668-9. PubMed PMID:
563 24221888.

564 37. Baldridge GD, Markowski TW, Witthuhn BA, Higgins L, Baldridge AS, Fallon AM. The
565 Wolbachia WO bacteriophage proteome in the *Aedes albopictus* C/wStr1 cell line: evidence for
566 lytic activity? *In Vitro Cell Dev Biol Anim*. 2016;52(1):77-88. Epub 2015/10/03. doi:
567 10.1007/s11626-015-9949-0. PubMed PMID: 26427709; PubMed Central PMCID:
568 PMCPMC4701759.

569 38. Charlat S, Hornett EA, Dyson EA, Ho PP, Loc NT, Schilthuizen M, et al. Prevalence and
570 penetrance variation of male-killing Wolbachia across Indo-Pacific populations of the butterfly
571 *Hypolimnas bolina*. *Mol Ecol*. 2005;14(11):3525-30. Epub 2005/09/15. doi: 10.1111/j.1365-
572 294X.2005.02678.x. PubMed PMID: 16156820.

573 39. Zweig M, Rosenkranz HS, Morgan C. Development of coliphage T5: ultrastructural and
574 biochemical studies. *J Virol*. 1972;9(3):526-43. Epub 1972/03/01. doi: 10.1128/JVI.9.3.526-
575 543.1972. PubMed PMID: 4259394; PubMed Central PMCID: PMCPMC356328.

576 40. Chauvatcharin N, Ahantarig A, Baimai V, Kittayapong P. Bacteriophage WO-B and
577 Wolbachia in natural mosquito hosts: infection incidence, transmission mode and relative
578 density. *Mol Ecol*. 2006;15(9):2451-61. Epub 2006/07/18. doi: 10.1111/j.1365-
579 294X.2006.02947.x. PubMed PMID: 16842419.

580 41. Sanogo YO, Dobson SL. WO bacteriophage transcription in Wolbachia-infected *Culex*
581 *pipiens*. *Insect Biochem Mol Biol*. 2006;36(1):80-5. Epub 2005/12/20. doi:
582 10.1016/j.ibmb.2005.11.001. PubMed PMID: 16360953.

583 42. Masui S, Kuroiwa H, Sasaki T, Inui M, Kuroiwa T, Ishikawa H. Bacteriophage WO and
584 virus-like particles in Wolbachia, an endosymbiont of arthropods. *Biochem Biophys Res
585 Commun*. 2001;283(5):1099-104. Epub 2001/05/18. doi: 10.1006/bbrc.2001.4906. PubMed
586 PMID: 11355885.

587 43. Lindsey ARI, Rice DW, Bordenstein SR, Brooks AW, Bordenstein SR, Newton ILG.
588 Evolutionary Genetics of Cytoplasmic Incompatibility Genes *cifA* and *cifB* in Prophage WO of
589 Wolbachia. *Genome Biol Evol*. 2018;10(2):434-51. Epub 2018/01/20. doi: 10.1093/gbe/evy012.
590 PubMed PMID: 29351633; PubMed Central PMCID: PMCPMC5793819.

591 44. Pichon S, Bouchon D, Liu C, Chen L, Garrett RA, Greve P. The expression of one
592 ankyrin *pk2* allele of the WO prophage is correlated with the Wolbachia feminizing effect in
593 isopods. *BMC Microbiol*. 2012;12:55. Epub 2012/04/14. doi: 10.1186/1471-2180-12-55.
594 PubMed PMID: 22497736; PubMed Central PMCID: PMCPMC3431249.

595 45. Boeckaerts D, Stock M, Criel B, Gerstmans H, De Baets B, Briers Y. Predicting
596 bacteriophage hosts based on sequences of annotated receptor-binding proteins. *Sci Rep*.
597 2021;11(1):1467. Epub 2021/01/16. doi: 10.1038/s41598-021-81063-4. PubMed PMID:
598 33446856; PubMed Central PMCID: PMCPMC7809048.

599 46. Braquart-Varnier C, Greve P, Felix C, Martin G. Bacteriophage WO in Wolbachia
600 infecting terrestrial isopods. *Biochem Biophys Res Commun*. 2005;337(2):580-5. Epub
601 2005/10/04. doi: 10.1016/j.bbrc.2005.09.091. PubMed PMID: 16198306.

602 47. Taylor MJ, Hoerauf A, Townson S, Slatko BE, Ward SA. Anti-Wolbachia drug discovery
603 and development: safe macrofilaricides for onchocerciasis and lymphatic filariasis. *Parasitology*.
604 2014;141(1):119-27. Epub 2013/07/23. doi: 10.1017/S0031182013001108. PubMed PMID:
605 23866958; PubMed Central PMCID: PMCPMC3884836.

606 48. Sullivan W. Vector Control: Wolbachia Expands Its Protective Reach from Humans to
607 Plants. *Curr Biol*. 2020;30(24):R1489-R91. Epub 2020/12/23. doi: 10.1016/j.cub.2020.11.005.
608 PubMed PMID: 33352133.

609 49. Royer S, Morais AP, da Fonseca Batistao DW. Phage therapy as strategy to face post-
610 antibiotic era: a guide to beginners and experts. *Arch Microbiol*. 2021. Epub 2021/01/22. doi:
611 10.1007/s00203-020-02167-5. PubMed PMID: 33474609.

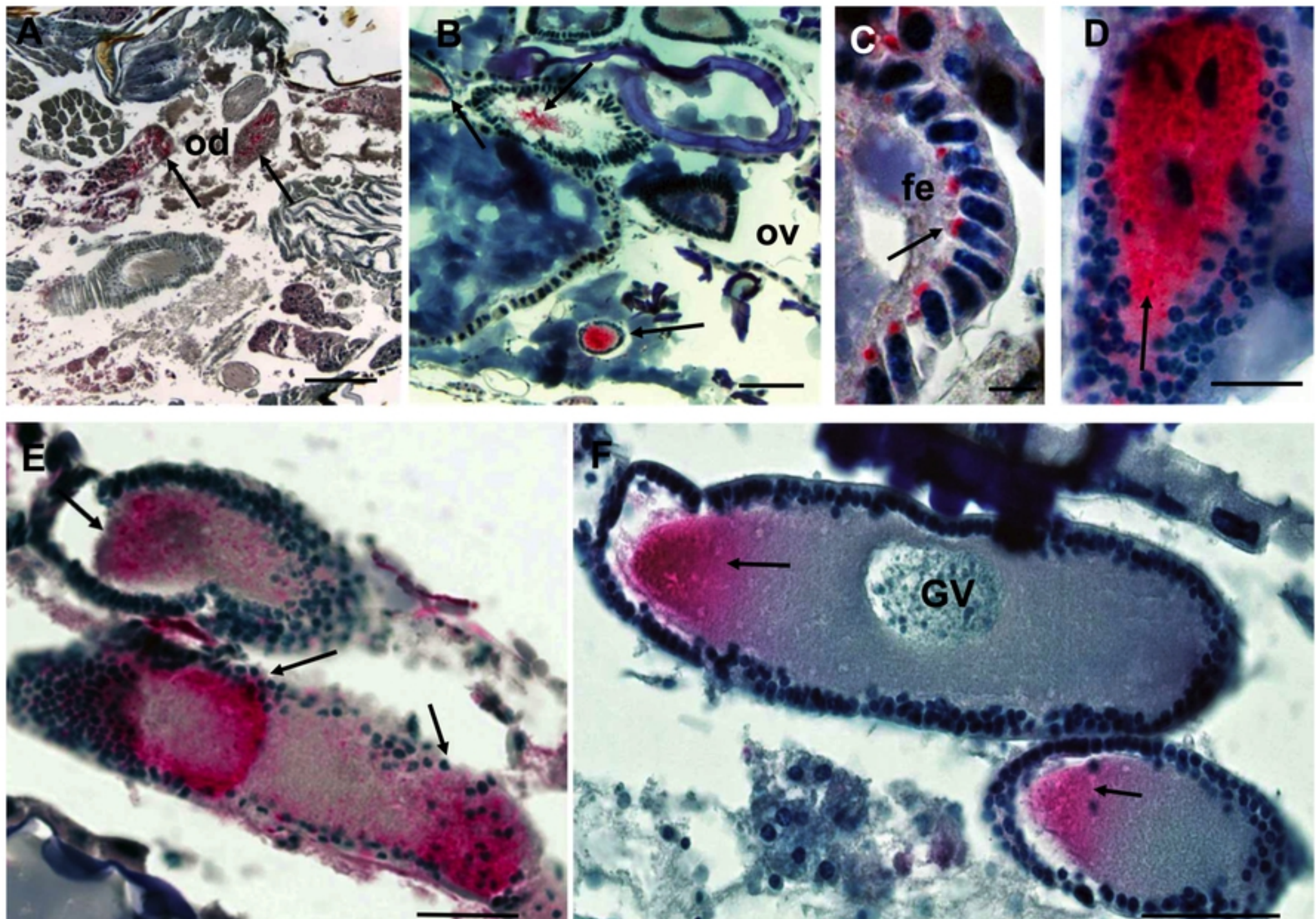


Figure 1

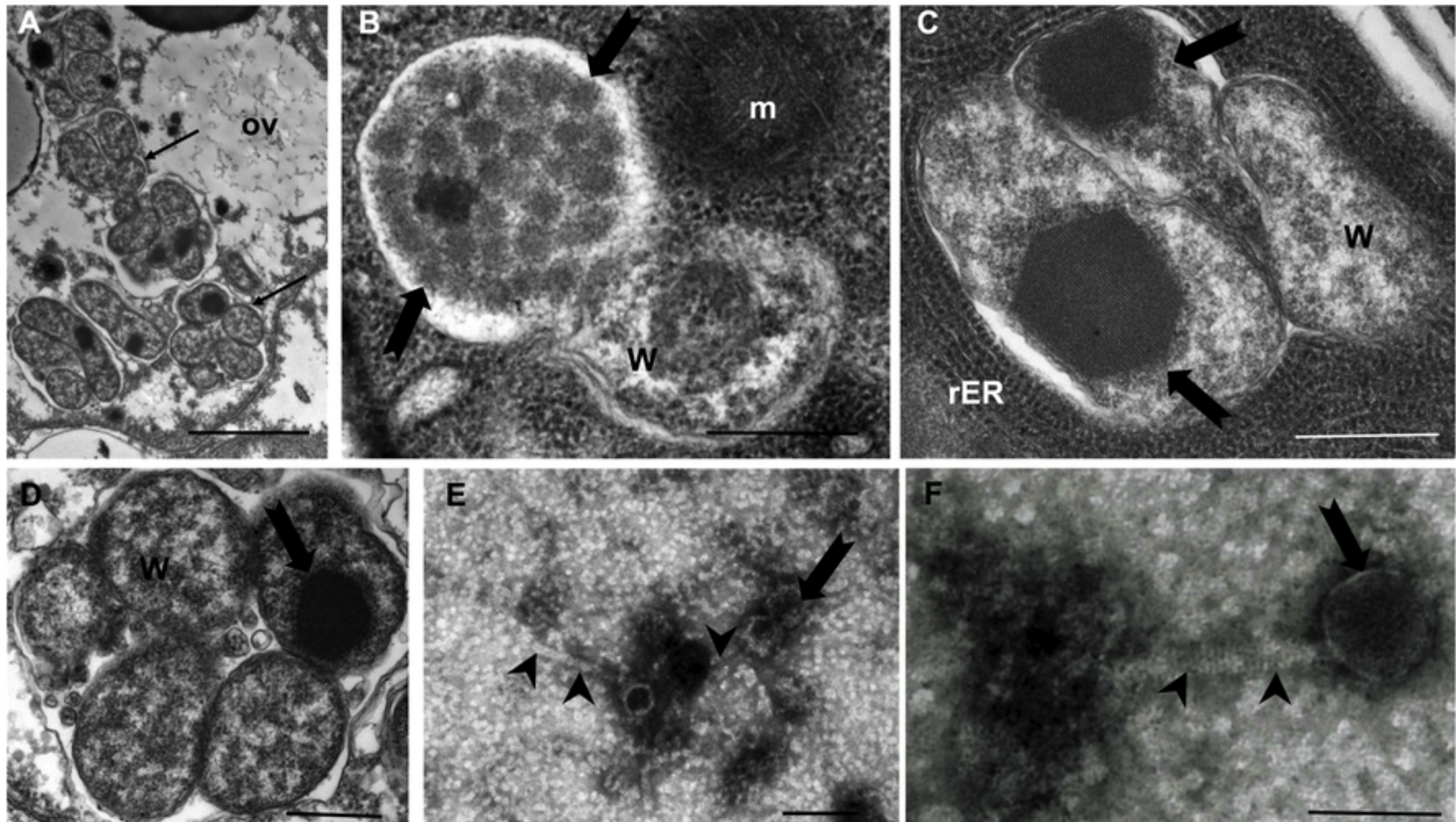


Figure 2

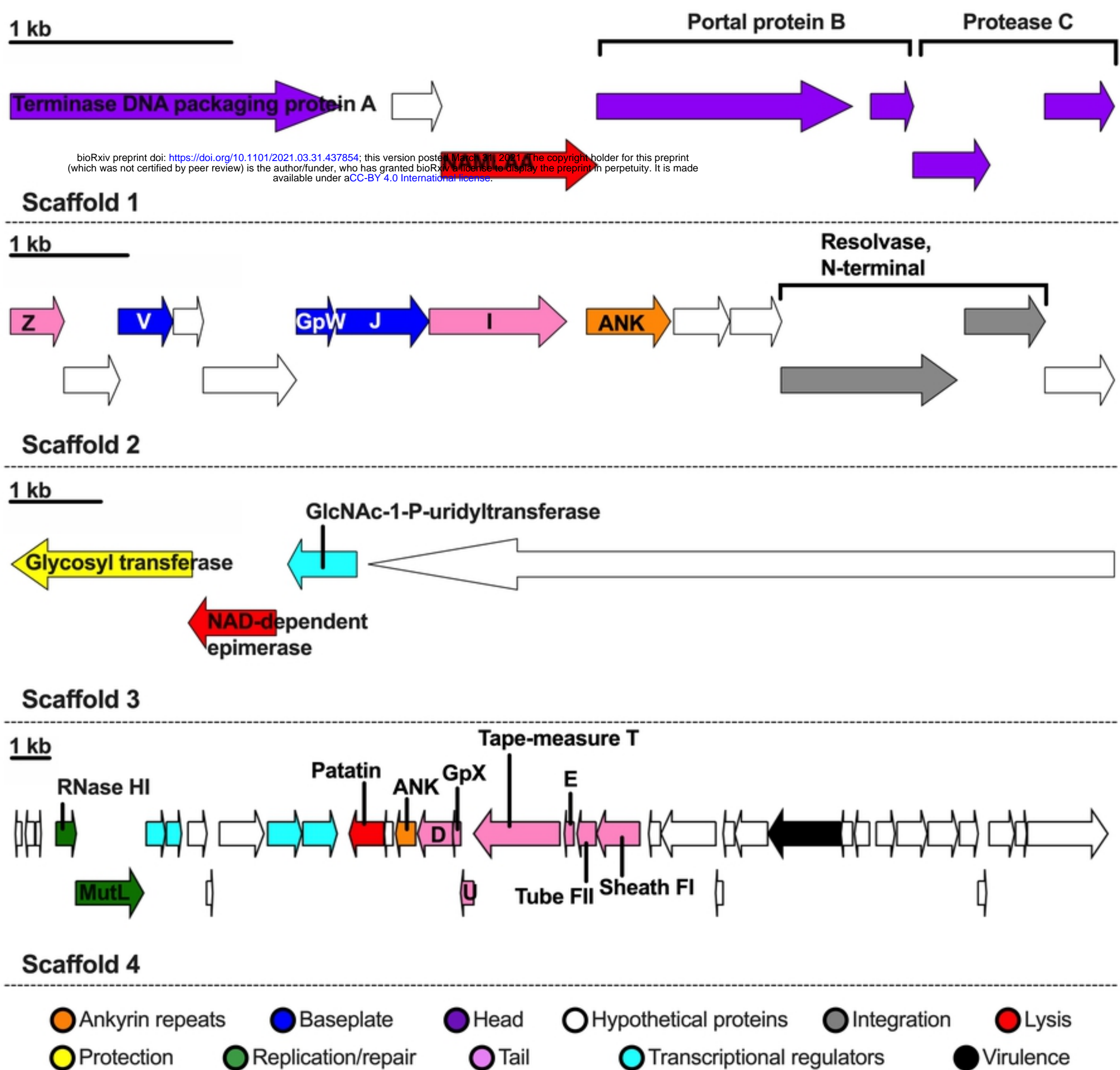


Figure3

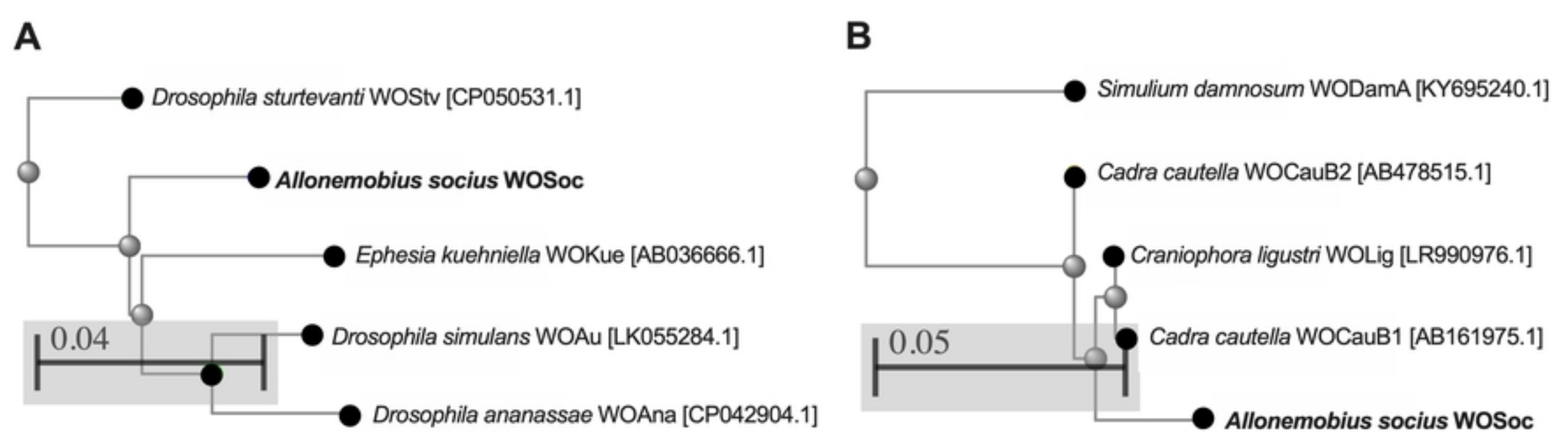


Figure4